JOC The Journal of Organic Chemistry

ARTICLE

pubs.acs.org/joc

Vicinal $^1H-^1H$ NMR Coupling Constants from Density Functional Theory as Reliable Tools for Stereochemical Analysis of Highly Flexible Multichiral Center Molecules

Fabian López-Vallejo,[†,‡] Mabel Fragoso-Serrano,[‡] Gloria Alejandra Suárez-Ortiz,[‡] Adriana C. Hernández-Rojas,[‡] Carlos M. Cerda-García-Rojas,[*,†] and Rogelio Pereda-Miranda[*,‡]

[†]Departamento de Química y Programa de Posgrado en Farmacología, Centro de Investigación y de Estudios Avanzados del Instituto Politécnico Nacional, A.P. 14-470, México, D. F. 07000 Mexico

[‡]Departamento de Farmacia, Facultad de Química, Universidad Nacional Autónoma de México, Circuito Exterior, Ciudad Universitaria, México, D. F. 04510 Mexico

Supporting Information

ABSTRACT: A protocol for stereochemical analysis, based on the systematic comparison between theoretical and experimental vicinal $^1H-^1H$ NMR coupling constants, was developed and applied to a series of flexible compounds (**1**−**8**) derived from the 6-heptenyl-5,6-dihydro-2*H*-pyran-2-one framework. The method included a broad conformational search, followed by geometry optimization at the DFT B3LYP/DGDZVP level, calculation of the vibrational frequencies, thermochemical parameters, magnetic shielding tensors, and the total NMR spin−spin coupling constants. Three scaling factors, depending on the carbon atom hybridizations, were found for the $^1H-C-C-^1H$ vicinal coupling constants: $f_{(sp3)-(sp3)} = 0.910$, $f_{(sp3)-(sp2)} = 0.929$, and $f_{(sp2)-(sp2)} = 0.977$. A remarkable correlation between the theoretical (J^{pre}) and experimental $^1H-^1H$ NMR (J^{exp}) coupling constants for spicigerolide (**1**), a cytotoxic natural product, and some of its synthetic stereoisomers (**2**−**4**) demonstrated the predictive value of this approach for the stereochemical assignment of highly flexible compounds containing multiple chiral centers. The stereochemistry of two natural 6-heptenyl-5,6-dihydro-2*H*-pyran-2-ones (**14** and **15**) containing diverse functional groups in the heptenyl side chain was also analyzed by application of this combined theoretical and experimental approach, confirming its reliability. Additionally, a geometrical analysis for the conformations of **1**−**8** revealed that weak hydrogen bonds substantially guide the conformational behavior of the tetraacyloxy-6-heptenyl-2*H*-pyran-2-ones.

INTRODUCTION

One of the most challenging tasks in the field of structure elucidation is stereochemical analysis performed on flexible organic compounds.[1] An accurate description of the three-dimensional arrangement is crucial for either synthesizing new bioactive substances or evaluating them in drug-receptor interaction models.[2] Theoretical NMR parameters have reached such a high level of accuracy that it is now possible for researchers to solve stereochemical problems in organic compounds.[3] For instance, the calculated $^1H-^1H$ vicinal coupling constants values ($^3J_{HH}$) are a powerful tool for the stereochemical analysis of complex molecules with multichiral centers, even in such cases of highly flexible compounds displaying a large number of conformers.[4]

Theoretical studies have focused mainly on proteins[5] and oligosaccharides,[6] as well as on polycyclic natural products with a restricted number of conformers.[7] In this study, a protocol for stereochemical analysis based on a systematic comparison between theoretical and experimental $^1H-^1H$ NMR vicinal coupling constants was developed and applied to a series of flexible compounds (**1**−**8**) (Figure 1) possessing a polyacylated chain with four contiguous stereocenters. This approach increases the number of theoretical protocols aimed at solving stereochemical aspects of flexible organic compounds as recently demonstrated by the use of ab initio NMR chemical shift calculations.[3]

Polyacylated 6-heptenyl-5,6-dihydro-2*H*-pyran-2-ones occur in several members of the mint family (Lamiaceae),[8] particularly in the genus *Hyptis*.[9,10] The pharmacological properties displayed by these natural molecules, e.g., antimicrobial, cytotoxic, and antitumoral activities,[8−10] make them an interesting subject for stereochemical exploration because all of them possess an α,β-unsaturated δ-lactone system, which is a well-known Michael acceptor. This moiety is the pharmacophoric group responsible for the cytotoxic properties of this type of compounds,[11] but conformational requirements for their interaction with target biomolecules have not yet been studied. These bioactive

Received: March 29, 2011
Published: June 21, 2011

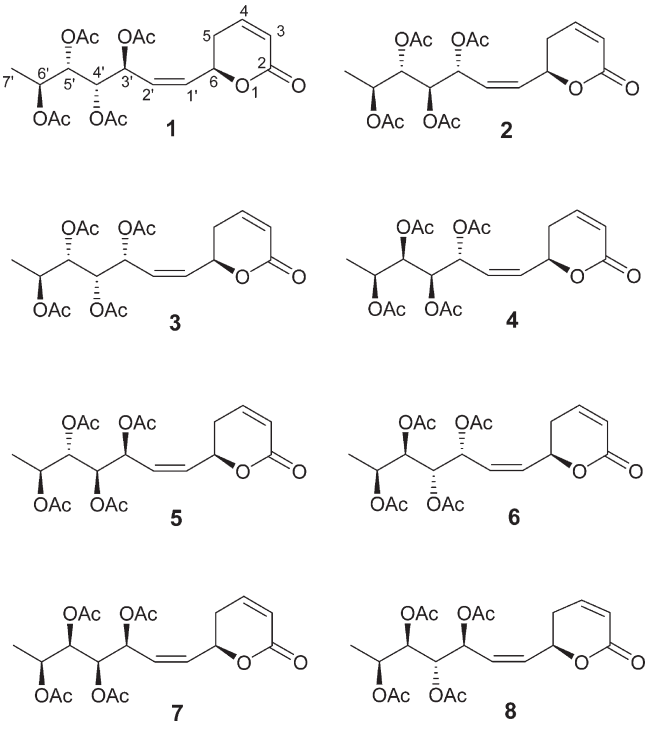

Figure 1. The eight possible stereoisomers for spicigerolide (**1**).

compounds are structurally related to pironetin, a pharmacologically relevant natural product that selectively binds to α-tubulin.[12] Preceding this report, the stereochemical elucidation of spicigerolide (**1**), a cytotoxic (KB, ED_{50} = 1.5 μg/mL) 6-tetraacetyloxyheptenyl-5,6-dihydro-2*H*-pyran-2-one, was determined by applying molecular mechanics and $^1H-^1H$ NMR coupling constant analysis (MM/$^3J_{HH}$) predicting the relative configuration for all its stereogenic centers.[10]

Current interest in this type of bioactive molecules has resulted in some synthetic approaches for **1** and several of its stereoisomers[13] since their cytotoxic potential strongly depends on the stereochemistry of the chiral centers located in both the pyrone moiety and the heptenyl side chain,[13a] which in any given compound governs its conformational arrangements leading to specific molecular geometries that selectively interact with bioreceptors. After comparing density functional theory calculations with experimental $^1H-^1H$ NMR coupling constants for the structural reassignment as well as stereochemical and conformation analysis of hypurticin,[4] another polyacylated 6-heptenyl-5,6-dihydro-2*H*-pyran-2-one, this approach was improved and resulted in the successful exploration of the full conformational space for eight diastereoisomers of spicigerolide (**1**−**8**) as described in this article. DFT scaling factors were found for the $^1H-C-C-^1H$ vicinal couplings ($^3J_{HH}$) augmenting the correlation between theoretical and experimental $^1H-^1H$ NMR coupling constants, emphasizing the efficacy of this method for stereochemical assignment of highly flexible compounds containing multiple chiral centers. Reliability of this approach was further confirmed when applied in the stereochemical analysis of two additional 6-heptenyl-5,6-dihydro-2*H*-pyran-2-ones containing diverse functional groups in the heptenyl side chain. The relevance of weak hydrogen bonds for the conformational behavior of tetraacyloxy-6-heptenyl-2*H*-pyran-2-ones was also elucidated.

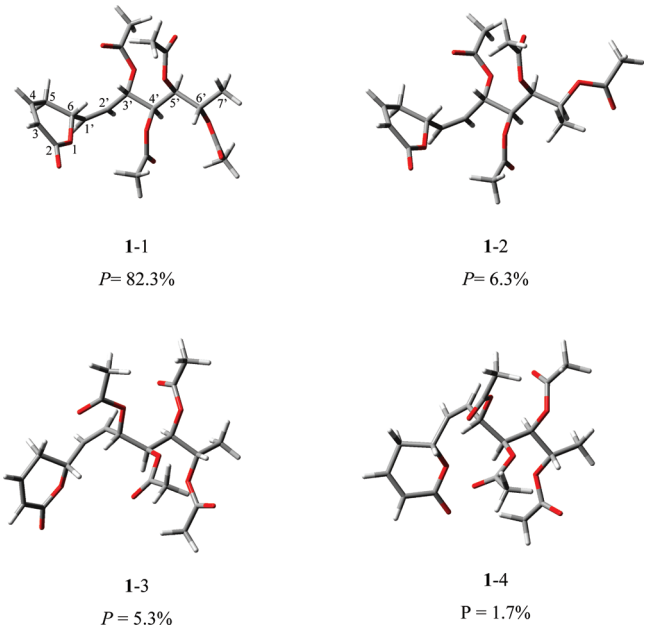

Figure 2. The four most relevant conformers of spicigerolide (**1**).

RESULTS AND DISCUSSION

A unique biogenetic feature of natural 6-heptenyl-5,6-dihydro-2*H*-pyran-2-ones is the (*S*)-configuration of the stereogenic center at C-6′.[9,12] This fact and the determination by circular dichroism of the (*R*)-configuration for the lactone C-6 chiral center[9,10] allow the possibility of eight diastereoisomers (**1**−**8**) for spicigerolide (Figure 1). Molecular mechanics was used for structure building and the initial conformational search for stereoisomers **1**−**8**. This systematic search used a protocol in which the torsion angles C(2′)−C(3′)−C(4′)−C(5′), C(3′)−C(4′)−C(5′)−C(6′), and C(4′)−C(5′)−C(6′)−C(7′) in the heptenyl moiety were rotated in steps of 120°, starting at 60° for each central bond. The torsion dihedral angles for C(1′)═C(2′)−C(3′)−C(4′) and C(5)−C(6)−C(1′)═C(2′) were rotated in steps of 180°. The acetyloxy $H-C_{sp3}-O-C_{sp2}$ and $C_{sp3}-O-C{=}O$ dihedral angles were initially set to 0° and explored within a range from +60° to −60°. A total of 108 initial conformers were generated for each of the eight stereoisomers. Due to severe intramolecular hindering steric interactions, a considerable number of conformers were discarded (see details in Experimental Section). The stable conformers were geometrically optimized, and their thermochemical parameters and IR frequencies were estimated. As an example, the four most relevant theoretical conformers of spicigerolide (**1**) are represented in Figure 2. For those conformers within the Gibbs free energy range of ΔG = 0−3 kcal/mol, the magnetic shielding tensors were calculated with the gauge-including atomic orbital (GIAO) method, followed by theoretical calculation of the total NMR spin−spin coupling constants (SSCC) at the B3LYP/DGDZVP level. The $\Delta G = -RT \ln K$ equation was used to obtain the population for each conformer taking into consideration a cyclic equilibrium among the selected conformers. Each coupling value was Boltzmann-weighted taking into account the DFT population to integrate the population-averaged coupling constants. Tables S1−S8 (Supporting Information) list the calculated values for the conformers of **1**−**8** ranging between 0 and 3 kcal/mol. As an example, IR frequencies and magnetic

dx.doi.org/10.1021/jo200637g |*J. Org. Chem.* 2011, 76, 6057–6066

Table 1. Summary[a] of Corrected[b] Weighted[c] Theoretical[d] ^{1}H−^{1}H Coupling Constants of Stereoisomers 1−8 and Experimental[e] *J*-values for 1−4

stereoisomer	J_{3-4}	J_{4-5S}	J_{4-5R}	J_{5S-6}	J_{5R-6}	$J_{6-1'}$	$J_{1'-2'}$	$J_{2'-3'}$	$J_{3'-4'}$	$J_{4'-5'}$	$J_{5'-6'}$
theor **1** (6*R*,3′*S*,4′*S*,5′*S*,6′*S*)	9.65	2.09	6.21	11.27	3.64	9.32	11.21	9.24	8.96	2.41	8.84
exp **1** (6*R*,3′*S*,4′*S*,5′*S*,6′*S*)	9.90	2.50	5.77	11.00	4.00	9.50	11.00	9.60	9.00	2.50	8.70
theor **2** (6*R*,3′*R*,4′*R*,5′*S*,6′*S*)	9.62	2.10	6.36	11.25	3.59	8.50	11.74	9.97	3.96	7.63	4.06
exp **2** (6*R*,3′*R*,4′*R*,5′*S*,6′*S*)	9.80	3.00	5.50	12.00	3.50	8.70	11.50	9.90	4.30	7.20	4.30
theor **3** (6*R*,3′*R*,4′*S*,5′*S*,6′*S*)	9.60	2.16	6.37	11.69	3.42	7.43	11.94	8.80	7.07	3.96	5.17
exp **3** (6*R*,3′*R*,4′*S*,5′*S*,6′*S*)	9.50	2.20	6.20	11.50	4.00	8.00	11.80	8.50	6.70	4.30	5.40
theor **4** (6*R*,3′*R*,4′*R*,5′*R*,6′*S*)	9.64	2.08	6.24	11.76	3.76	7.35	11.46	9.62	6.94	3.97	6.99
exp **4** (6*R*,3′*R*,4′*R*,5′*R*,6′*S*)	10.00	3.00	5.50	11.40	4.20	8.10	11.50	10.00	6.80	4.00	7.20
theor **5** (6*R*,3′*S*,4′*R*,5′*S*,6′*S*)	9.65	2.09	6.29	11.23	3.70	9.04	11.52	9.84	7.26	3.46	5.26
theor **6** (6*R*,3′*R*,4′*S*,5′*R*,6′*S*)	9.63	2.12	6.26	11.91	3.59	6.81	11.81	9.55	2.85	9.23	2.60
theor **7** (6*R*,3′*S*,4′*R*,5′*R*,6′*S*)	9.64	2.09	6.27	11.24	3.73	9.10	11.45	9.49	5.56	4.49	5.11
theor **8** (6*R*,3′*S*,4′*S*,5′*R*,6′*S*)	9.63	2.09	6.24	11.39	3.68	8.72	11.30	9.16	8.62	2.04	8.07

[a] For full details on theoretical coupling constant calculations for each contributing conformer, see Supporting Information (Tables S1−S8). [b] The scaling factors were as follows: $f_{H(sp3)-H(sp3)}$= 0.910; $f_{H(sp3)-H(sp2)}$=0.929 and $f_{H(sp2)-H(sp2)}$ = 0.977. [c] Boltzmann averaged with equation $\Sigma_i J^i \times P^i$, where J^i is the spin−spin coupling constant value (in Hz) for each conformer and P^i is the population for the *i*th conformation calculated from $\Delta G°$ values at 298 K and 1 atm. [d] Obtained from the DFT optimized structures at the B3LYP/DGDZVP level. [e] In Hz, obtained by nonlinear fit of the experimental ^{1}H NMR spectrum to the simulated spectrum generated by iteration of spectral parameters (^{1}H chemical shifts, *J*-couplings, and line width).

shield tensors for spicigerolide (**1**) selected conformers are included in Tables S13−S30 in Supporting Information, and the corresponding H−C−C−H dihedral angles are listed in Table S31.

Theoretical ^{1}H−^{1}H coupling constants values for compounds **1**−**8** are summarized in Table 1, where experimental $^3J_{HH}$ values for compounds **1**−**4** were also included for comparison to determine the accuracy of the calculations. Through the nonlinear fit of the ^{1}H NMR spectrum to the spectral parameters obtained by iterative processing, the accurate experimental $^3J_{HH}$ values were obtained for an authentic sample of spicigerolide (**1**)[10] and for derivatives **2**−**4** (Table 2). Compounds **1**−**4** displayed distinctive $^3J_{HH}$ coupling constant values that correlated with their configurational arrangement (Figures S1−S4, Supporting Information).

Figure 3 shows the synthetic sequence for the microscale preparation of diastereoisomers **2**−**4**. Acetylation of synrotolide (**9**), isolated from a member of the mint family found only in Pondoland, South Africa[14] afforded the peracetylated derivative **2** and the triacetylated compounds **10** and **11**, both of which were used for the epimerization of chiral centers C-4′ and C-5′, respectively. Jones' oxidation of alcohols **10** and **11** afforded ketones **12** and **13**, which were then subjected to hydride reduction and acetylation to yield diasteroisomers **3** and **4**, respectively. Regeneration of compound **2** was also observed.

The differences between the experimental and calculated coupling constants of **1**−**4** (Table 1) were estimated by root-mean-square deviation values (rmsd). All calculations were carried out with neither solvation effects nor intermolecular interactions but including the inherent approximations of the quantum methods. Three scaling factors (*f*)[15] were calculated to compensate for the slightly overestimated $^3J_{HH}$ values: $J^{pre} = f_x J^{calc}$, arising from the limitations of the employed theoretical methods and which may compensate for the approximations inherent in the quantum mechanics equations for a given structure, as has been reported in work related to coupling constants.[15] Each factor was determined by an iterative process structured to minimize the global rmsd. The procedure took into account the whole set of calculated versus experimental $^3J_{HH}$ values, which were grouped according to the carbon atom hybridization of the H−C−C−H fragments as follow: $f_{H(sp3)-H(sp3)}$ = 0.910; $f_{H(sp3)-H(sp2)}$ = 0.929, and $f_{H(sp2)-H(sp2)}$ = 0.977. For compounds **1**−**4**, the rmsd values before applying the scaling factors were 0.70, 0.72, 0.69, and 0.73 Hz, respectively, taking into account the whole set of vicinal coupling constants. When using the scaling factors, these numbers substantially decreased to 0.26, 0.50, 0.34, and 0.48 Hz. If the comparison focuses on the coupling constants arising from the C(3′)−C(4′)−C(5′)−C(6′) fragment ($J_{3'-4'}$, $J_{4'-5'}$, and $J_{5'-6'}$), where the stereochemical differences take place along the series of 6-heptenyl-5,6-dihydro-2*H*-pyran-2-ones, the rmsd values decrease even more considerably. For compounds **1**−**4**, these values were only 0.10, 0.35, 0.32, and 0.15, respectively. The complete set of rmsd comparative values, including the theoretical coupling constants of **5**−**8**, is shown in Figure 4.

Convergence between DFT calculated and experimental ^{1}H−^{1}H NMR coupling constant values in the four diastereoisomers **1**−**4** (Table 1) arises from the following results: (1) the exact calculation for each conformer's geometry; (2) the precise estimation of the free energies and Boltzmann population for each analyzed stereoisomer; and (3) the appropriate selection of the coupling constant calculation method, as in this case B3LYP/DGDZVP. This approach provides a single and specific solution for each set of $^3J_{HH}$ values for diastereoisomers **1**−**4**, resulting in the stereochemical assignment for each chiral center present in the flexible moiety of each analyzed structure, as well as in the conformational behavior of the entire molecule. In the present study, the use of solvent models was excluded since the contribution to *J* is generally low in molecules lacking polar protic fuctional groups as OH, NH, and/or COOH, when dissolved in $CDCl_3$, an aprotic solvent with a relatively low dipolar moment.

Two natural products (**14** and **15**, Figure 5) containing the 6-heptenyl-5,6-dihydro-2*H*-pyran-2-one framework, but with diverse functional groups in the heptenyl side chain, were also subjected to the same combined theoretical and experimental methodology as a test for its reliability. The conformational search, minimization procedures, and coupling constant calculations were

dx.doi.org/10.1021/jo200637g |*J. Org. Chem.* 2011, 76, 6057–6066

Table 2. Experimental ^{1}H NMR Chemical Shifts, Multiplicities, and $^3J_{HH}$ Coupling Constants of Compounds 1−4[a]

H	1	2	3	4
3	6.06 ddd ($J_{3,4}$ = 9.90, $J_{3,5ax}$ = −2.75, $J_{3,5eq}$ = −1.10)	6.06 ddd ($J_{3,4}$ = 9.80, $J_{3,5ax}$ = −2.20, $J_{3,5eq}$ = −1.40)	6.06 ddd ($J_{3,4}$ = 9.50, $J_{3,5ax}$ = −2.50, $J_{3,5eq}$ = −1.50)	6.07 ddd ($J_{3,4}$ = 10.00, $J_{3,5ax}$ = −2.20, $J_{3,5eq}$ = −1.40)
4	6.90 ddd ($J_{4,3}$ = 9.90, $J_{4,5ax}$ = 2.50, $J_{4,5eq}$ = 5.77)	6.90 ddd ($J_{4,3}$ = 9.80, $J_{4,5ax}$ = 3.00, $J_{4,5eq}$ = 5.50)	6.88 ddd ($J_{4,3}$ = 9.50, $J_{4,5ax}$ = 2.20, $J_{4,5eq}$ = 6.20)	6.90 ddd ($J_{4,3}$ = 10.00, $J_{4,5ax}$ = 3.00, $J_{4,5eq}$ = 5.50)
5ax	2.35 dddd ($J_{5ax,5eq}$ = −18.50, $J_{5ax,6}$ = 11.00, $J_{5ax,3}$ = −2.75, $J_{5ax,4}$ = 2.50)	2.43 dddd ($J_{5ax,5eq}$ = −17.40, $J_{5ax,6}$ = 12.00, $J_{5ax,3}$ = −2.2, $J_{5ax,4}$ = 3.00)	2.49 dddd ($J_{5ax,5eq}$ = −18.50, $J_{5ax,6}$ = 11.50, $J_{5ax,3}$ = −2.50, $_{5ax,4}$ = 2.20)	2.35 dddd ($J_{5ax,5eq}$ = −17.10, $J_{5ax,6}$ = 11.40, $J_{5ax,3}$ = −2.20, $J_{5ax,4}$ = 3.00)
5eq	2.52 dddd ($J_{5eq,5ax}$ = −18.50, $J_{5eq,4}$ = 5.77, $J_{5eq,6}$ = 4.00, $J_{5eq,3}$ = −1.10)	2.43 dddd ($J_{5eq,5ax}$ = −17.40, $J_{5eq,4}$ = 5.50, $J_{5eq,6}$ = 3.50, $J_{5eq,3}$ = −1.40)	2.36 dddd ($J_{5eq,5ax}$ = −18.50, $J_{5eq,4}$ = 6.20, $J_{5eq,6}$ = 4.00, $J_{5eq,3}$ = −1.50)	2.52 dddd ($J_{5eq,5ax}$ = −17.10, $J_{5eq,4}$ = 5.50, $J_{5eq,6}$ = 4.20, $J_{5eq,3}$ = −1.40)
6	5.35 dddd ($J_{6,1'}$ = 9.50, $J_{6,5ax}$ = 11.00, $J_{6,5eq}$ = 4.00, $J_{6',2'}$ = −0.90)	5.30 dddd ($J_{6,1'}$ = 8.70, $J_{6,5ax}$ = 12.00, $J_{6,5eq}$ = 3.50, $J_{6,2'}$ = −1.00)	5.30 dddd ($J_{6,1'}$ = 8.00, $J_{6,5ax}$ = 11.50, $J_{6,5eq}$ = 4.00, $J_{6,2'}$ = −1.10)	5.38 dddd ($J_{6,1'}$= 8.10, $J_{6,5ax}$ = 11.40, $J_{6,5eq}$ = 4.20, $J_{6,2'}$ = −1.50)
1′	5.79 dd ($J_{1',2'}$ = 11.00, $J_{1',6'}$ = 9.50)	5.87 ddd ($J_{1',2'}$ = 11.50, $J_{1',6}$ = 8.70, $J_{1',3'}$ = −0.85)	5.80 ddd ($J_{1',2'}$ = 11.80, $J_{1',6}$ = 8.00, $J_{1',3'}$ = −0.50)	5.90 ddd ($J_{1',2'}$ = 11.50, $J_{1',6}$ = 8.10, $J_{1',3'}$ = −1.00)
2′	5.49 ddd ($J_{2',1'}$ = 11.00, $J_{2',3'}$ = 9.60, $J_{2',6}$ = −0.90)	5.64 ddd ($J_{2',1'}$ = 11.50, $J_{2',3'}$ = 9.90, $J_{2',6}$ = −1.00)	5.56 ddd ($J_{2',1'}$ = 11.80, $J_{2',3'}$ = 8.50, $J_{2',6}$ = −1.10)	5.63 ddd ($J_{2',1'}$ = 11.50, $J_{2,3'}$ = 10.00, $J_{2',6}$ = −1.50)
3′	5.40 dd ($J_{3',2'}$ = 9.60, $J_{3',4'}$ = 9.00)	5.69 ddd ($J_{3',2'}$ =9.80, $J_{3',4'}$ = 4.30, $J_{3',1'}$ = −0.85)	5.70 ddd ($J_{3',2'}$ = 8.5, $J_{3',4'}$ = 6.70, $J_{3',1'}$ = −0.50)	5.50 ddd ($J_{3',2}$ =10.00, $J_{3',4'}$ = 6.80, $J_{3',1'}$ = −1.00)
4′	5.37 dd ($J_{4',3'}$ = 9.00, $J_{4',5'}$ = 2.50)	5.25 dd ($J_{4',5'}$ = 7.20, $J_{4',3'}$ = 4.30)	5.33 dd ($J_{4',3'}$ = 6.70, $J_{4',5'}$ = 4.30)	5.32 dd ($J_{4',3'}$ = 6.80, $J_{4',5'}$ = 4.00)
5′	5.30 dd ($J_{5',6'}$ = 8.70, $J_{5',4'}$ = 2.50)	5.17 dd ($J_{5',4'}$ = 7.20, $J_{5',6'}$ = 4.30)	5.23 dd ($J_{5',6'}$ = 5.40, $J_{5',4'}$ = 4.30)	5.21 dd ($J_{5',6'}$ = 7.20, $J_{5',4'}$ = 4.00)
6′	4.96 dq ($J_{6',5'}$ = 8.70, $J_{6',7'}$ = 6.30)	5.10 dq ($J_{6',7'}$ = 6.50, $J_{6',5'}$ = 4.30)	4.98 dq ($J_{6',5'}$ = 5.40, $J_{6',7'}$ = 6.50)	4.98 dq ($J_{6',5'}$ = 7.20, $J_{6',7'}$ = 6.50)
Me-7′	1.19 d ($J_{7',6'}$ = 6.30)	1.22 d ($J_{7',6'}$ = 6.50)	1.24 d ($J_{7',6'}$ = 6.50)	1.21 d ($J_{7',6'}$ = 6.50)
OAc	2.12 s, 2.12 s, 2.04 s, 2.03 s	2.11 s, 2.11 s, 2.06 s, 2.03 s	2.12 s, 2.09 s, 2.09 s, 2.02 s	2.10 s, 2.08 s, 2.05 s, 2.03 s

[a] Obtained by nonlinear fit of the experimental ^{1}H NMR spectrum to the simulated spectrum generated by iteration of spectral parameters (^{1}H chemical shifts, *J*-couplings, and line width).

dx.doi.org/10.1021/jo200637g | *J. Org. Chem.* 2011, 76, 6057–6066

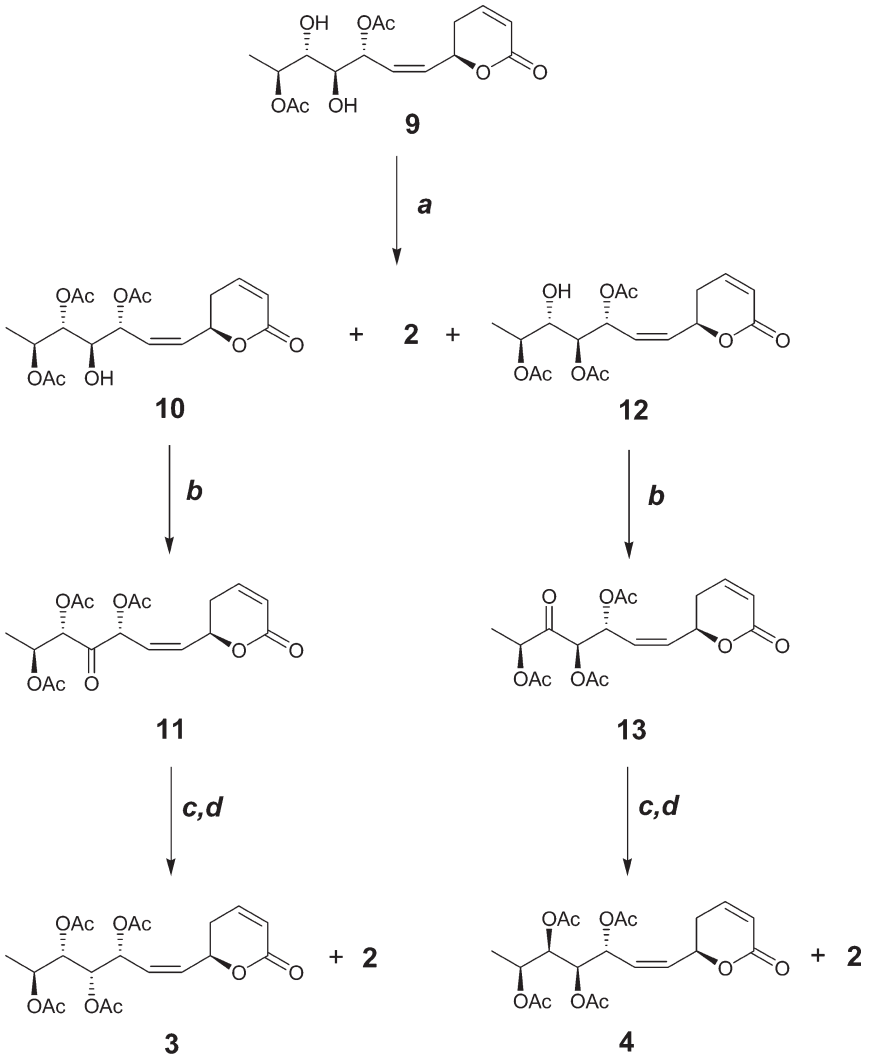

a. Ac_2O/Pyridine (-10 °C for 60 min then 25 °C for 180 min).
b. CrO_3 in H_2O/AcOH.
c. $NaBH_4$ in MeOH.
d. AcCl.

Figure 3. Epimerization reactions of synrotolide (**9**).

obtained for the molecular models of 5′-*epi*-olguine (**14**)[21] and its 5-deacetoxy derivative (**15**)[22] (Figures S5 and S6, Supporting Information) as described above for spicigerolide (**1**) and stereoisomers (**2**−**8**) while the experimental values (Table 3) were also obtained by nonlinear fit of the ^{1}H NMR spectrum to the spectral parameters (Figures S7 and S8, Supporting Information). The calculated Boltzmann-averaged vicinal coupling constants found in the whole alkenyl chain were contrasted with the experimental ones summarized in Table 4 (see also Tables S9−S12, Supporting Information) giving rmsd of 0.25 Hz for **14** and 0.45 Hz for **15**. After the chiral center at C-5′ in both structures (**14** and **15**) was inverted for the formulation of their epimeric compounds, molecular models for olguine (**16**)[23] and its hypothetic deacetoxy derivative **17** were generated, respectively. Once the calculation procedures were applied, taking into account the incorrect alternative structures, the rmsd values for the complete set of couplings substantially increased up to 2.82 for **16** and 1.23 Hz for **17** for the whole chain (Table 4). Additionally, if the comparison is focused on the coupling constants at the C(4′)−C(5′)−C(6′) fragment, where the differences between **14** and **16** or between **15** and **17** are found due to the change in chirality at C-5′, the rmsd for the correct structures decreases to 0.03 Hz for **14** and 0.21 Hz for **15**. In contrast, inversion of the chirality at C-5′ to generate the incorrect stereoisomers causes this value to increase to 3.87 for **16** and 2.02 Hz for **17** (Table 4). The agreement between theoretical and experimental values for the stereochemically correct structures, indicated by small rmsd values, in conjunction with large rmsd values for the incorrect stereoisomers, demonstrated the efficacy of this computational protocol based on DFT ^{1}H−^{1}H NMR coupling constant calculations as a stereochemical analytical tool to aid in structure elucidation of flexible organic

dx.doi.org/10.1021/jo200637g |*J. Org. Chem.* 2011, 76, 6057–6066

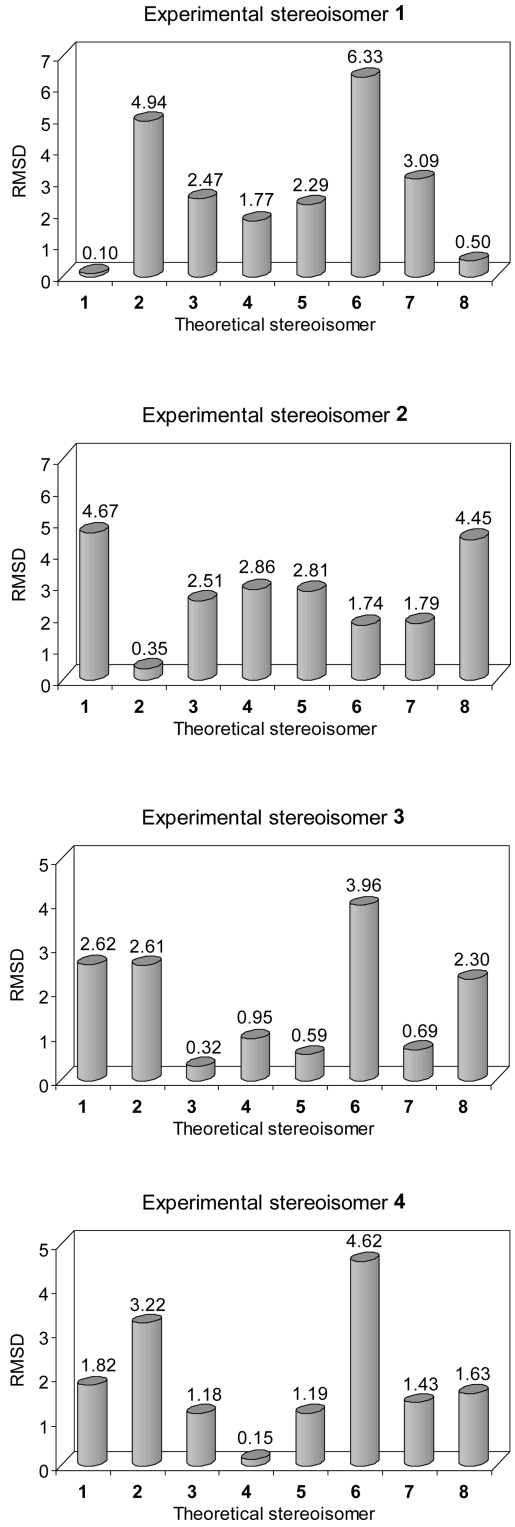

Figure 4. Comparison between experimental (**1**−**4**) and theoretical (**1**−**8**) coupling constants values using rmsd statistics. In the four cases, the minimum rmsd value is found when the correct theoretical stereoisomer matches the experimental one.

synthetic molecules and natural products with multiple chiral centers.

A fundamental task in molecular modeling of highly flexible compounds is the accurate estimation of their conformational

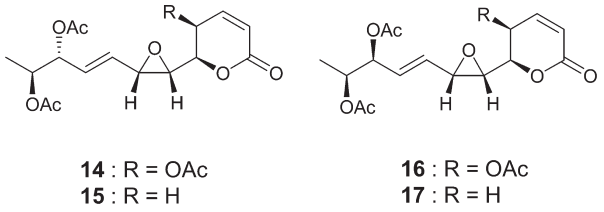

14 : R = OAc
15 : R = H

16 : R = OAc
17 : R = H

Figure 5. Structures of 5′-*epi*-olguine (**14**), olguine (**16**), and their 5-deacetoxy derivatives (**15** and **17**).

distribution. In the case of peracetylated acyclic derivatives of sugars, coplanar and fully extended *zigzag* conformations, but with exclusion of 1,3-parallel nonbonded oxygen−oxygen interactions, constitute the major contribution to their conformational equilibrium.[16] Analysis of the tridimensional structures of **1**−**4** revealed the presence of a few 1,3-oxygen−oxygen interactions and many weak hydrogen bonds, both factors playing an important role in their conformational behavior. The study of weak hydrogen bonds has been an area of intense discussion over recent years in organic structural chemistry, structural biology, and medicinal chemistry.[17] Experimental and theoretical evidence have confirmed that these bonds play important roles in the conformational behavior of organic molecules, in molecular recognition, and in the supramolecular architectures. Two of the above-mentioned interactions are presented in conformers **1**-1 and **1**-2 (Figure 2). Notably, the first weak hydrogen bond was established between the oxygen of the lactone group and the hydrogen atoms of the acetyloxy moiety at C-4′ in both cases. The second was formed between the hydrogen atoms of the acetyloxy moiety at C-3′ and the oxygen atom of carbonyl group at C-5′. Conformer **1**-3 also displayed two interactions of this type but established between different pairs of atoms. The first interaction was found between the acidic *pseudo*-equatorial hydrogen at C-5 on the lactone ring and the carbonyl group of the acetyloxy moiety at C-3′. The second, between the vinylic hydrogen at C-2′ and the carbonyl group of the acetyloxy moiety at C-5′. These weak hydrogen bonds were observed in the majority of the analyzed conformers of **1**−**4**. From 141 intramolecular C−H···O interactions (Figure 6) observed in 71 conformers (Tables S1−S4 in Supporting Information), a total of 17 were established between acetyl methyl hydrogen atoms and the lactone carbonyl oxygen. The more populated weak hydrogen interactions corresponded to those between the *pseudo*-equatorial allylic hydrogen H-5 and the acetyl carbonyl oxygens, totaling 47. In eight cases, vinylic hydrogens H-1′ or H-2′ were found to interact with the acetyl carbonyl oxygen atoms located in the heptenyl side chain; in six cases, acetyl methyl hydrogen atoms presented weak hydrogen bonds with the lactone ether oxygen. Interactions between acetyl methyl hydrogen atoms and acetyl carbonyl oxygen took place 24 times with the second most frequent interaction occurring between allylic hydrogen H-6 and acetyl carbonyl or ether oxygen atoms, totaling 26. Finally, allylic hydrogen H-3′ interacted with acetyl carbonyl oxygen atoms or the lactone ether oxygen in 13 occasions.

As observed in several polyoxygenated compounds,[18] two main factors that characterize weak hydrogen bonds are the distance between the two interacting atoms H···O, which must be shorter than the sum of their van der Waals radii (2.72 Å), and the C−H···O bond angles, which trend toward 180°. Figure 6 shows the scatter plot of C−H···O angles versus O···H

dx.doi.org/10.1021/jo200637g |*J. Org. Chem.* 2011, 76, 6057–6066

Table 3. Experimental ^{1}H NMR Chemical Shifts, Multiplicities, and $^3J_{HH}$ Coupling Constants for the Alkenyl Chain of 5′-*epi*-Olguine (14) and 5-Deacetoxy-5′-*epi*-olguine (15)[a]

H	14	15
6	4.19 dd ($J_{5,6}$ = 2.94 $J_{6,1'}$ = 8.40)	4.18 ddd ($J_{5proR,6}$ = 7.80, $J_{5proS,6}$ = 6.0, $J_{6,1'}$ = 8.20)
1′	3.49 dd ($J_{6,1'}$ = 8.40, $J_{1',2'}$ = 4.03)	3.32 dd ($J_{6,1'}$ = 8.20, $J_{1',2'}$ = 4.10)
2′	3.68 dd ($J_{1',2'}$ = 4.03, $J_{2',3'}$ = 4.36)	3.60 dd ($J_{1',2'}$ = 4.10, $J_{2',3'}$ = 5.20)
3′	5.78 dd ($J_{2',3'}$ = 4.36, $J_{3',4'}$ = 15.6)	5.78 dd ($J_{2',3'}$ = 5.20, $J_{3',4'}$ = 15.80)
4′	5.86 dd ($J_{3',4'}$ = 15.6, $J_{4',5'}$ = 5.70)	5.87 dd ($J_{3',4'}$ = 15.80, $J_{4',5'}$ = 6.30)
5′	5.33 dd ($J_{4',5'}$ = 5.70, $J_{5',6'}$ = 3.60)	5.35 dd ($J_{4,5'}$ = 6.30, $J_{5',6'}$ = 4.10)
6′	5.06 dq ($J_{5',6'}$ = 3.60, $J_{6',7'}$ = 6.30)	5.07 dq ($J_{5',6'}$ = 4.10, $J_{6',7'}$ = 6.40)
Me-7′	1.16 d ($J_{6',7'}$ = 6.30)	1.18 d ($J_{6',7'}$ = 6.40)
OAc	2.03 s, 2.07 s, 2.14 s	2.04 s, 2.09 s

[a] Obtained by nonlinear fit of the experimental ^{1}H NMR spectrum to the simulated spectrum generated by iteration of spectral parameters (^{1}H chemical shifts, *J*-couplings, and line width).

Table 4. Comparison between Theoretical and Experimental ^{1}H−^{1}H Coupling Constants for Compounds 14 and 15 in Contrast with Their C-5′ Epimers 16 and 17

compound	$J_{6,1'}$	$J_{1',2'}$	$J_{2',3'}$	$J_{3',4'}$	$J_{4',5'}$	$J_{5',6'}$	rmsd[a]	rmsd[b]
theor **14**[c]	8.73	3.51	4.34	15.63	5.68	3.64	0.25[d]	0.03[d]
exp **14**[e]	8.40	4.03	4.36	15.60	5.70	3.60		
theor **16**[c]	8.78	3.54	8.52	15.55	8.49	8.31	2.82[f]	3.87[f]
theor **15**[c]	8.71	3.42	5.83	15.64	6.57	4.22	0.45[d]	0.21[d]
exp **15**[e]	8.20	4.10	5.20	15.80	6.30	4.10		
theor **17**[c]	8.56	3.40	5.59	15.41	7.73	6.58	1.23[f]	2.02[f]

[a] RMDS for the whole set of coupling constants. [b] RMDS for the coupling constants around the inverted chiral center at C-5′ ($J_{4',5'}$ and $J_{5',6'}$). [c] Theoretical coupling constants in Hz calculated from the B3LYP/DGDZVP structures and Boltzmann averaged using the equation $\Sigma_i J^i \times P^i$, where J^i is the coupling constant value for each conformer and P^i is the population for the *i*th conformation (for full details see Supporting Information). The coupling constants were scaled with factors: $f_{H(sp3)-H(sp3)}$ = 0.910; $f_{H(sp3)-H(sp2)}$ = 0.929, and $f_{H(sp3)-H(sp3)}$ = 0.977. [d] Small rmsd value denotes correct stereoisomer. [e] In Hz, obtained by nonlinear fit of the experimental ^{1}H NMR spectrum to the simulated spectrum generated by iteration of spectral parameters (^{1}H chemical shifts, *J*-couplings, and line width). [f] Large rmsd value denotes incorrect stereoisomer.

distances, each dot representing a weak hydrogen bond measured in the DFT structures of **1**−**4**. The minimum observed O···H distance was 2.33 Å in the present study, and a cutoff of 2.80 Å from previously described analysis was selected.[19] For C−H···O bond angles, which ranged between 110° and 180°, an evident C−H directionality was observed toward a maximum frequency between 150° and 160° weighted with 1/sin θ as reported by Kroon.[20] A shorter interaction had a higher angle value as shown by the plotted values in Figure 6.

These preliminary results indicate that a detailed qualitative study of weak hydrogen bonds in polyketide structures, such as **1**−**8**, merits further investigation because such interactions may play a relevant role in the conformational equilibrium of many bioactive substances. Conformers **1**-3 and **1**-4 (Figure 2) are representative examples of significant local minima where stabilizing weak hydrogen bonds coexist with the destabilizing 1,3 oxygen−oxygen interactions present in the O(3)−C(3)−C(4)−C(5)−O(5) fragment.

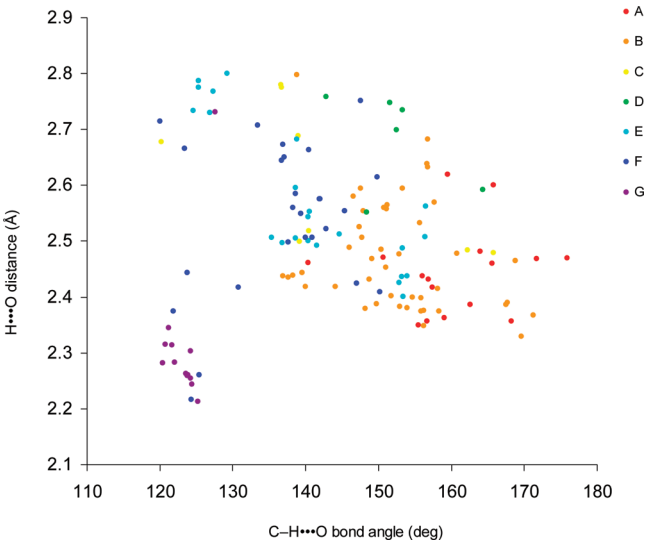

Figure 6. Scatter plot of C−H···O bond angles versus H···O distances for weak hydrogen bonds between (A) acetyl methyl hydrogens and lactone carbonyl oxygen; (B) the allylic hydrogen H-5$_{eq}$ and acetyl carbonyl oxygens; (C) vinylic hydrogens H-1′ or H-2′ and acetyl carbonyl oxygens; (D) acetyl methyl hydrogens and lactone ether oxygen; (E) acetyl methyl hydrogens and acetyl carbonyl oxygens; (F) allylic hydrogen H-6 and acetyl carbonyl or ether oxygens; and (G) allylic hydrogen H-3′ and acetyl carbonyl oxygens or lactone ether oxygen.

CONCLUSIONS

Stereochemical issues are subtle points in the structural assignment of active principles where a single inversion on the absolute stereochemistry of a chiral center could be responsible for the lack of biological activity, as previously demonstrated for spicigerolide (**1**) and some of its diastereoisomers. Therefore, the presented protocol for stereochemical analysis, based on the convergence between DFT calculated and experimental vicinal ^{1}H−^{1}H NMR coupling constants, can be of great utility as a predictive tool in the stereochemical assignment of chiral centers of biodynamic flexible polyketides. It also can be concluded that in 6-heptenyl-5,6-dihydro-2*H*-pyran-2-ones, weak hydrogen bonds may counterbalance the destabilizing effect of 1,3-oxygen−oxygen interactions present in some minimum energy conformers.

dx.doi.org/10.1021/jo200637g |*J. Org. Chem.* 2011, 76, 6057–6066

EXPERIMENTAL SECTION

General. All melting points are uncorrected. Optical rotations were measured using a microcell of l = 1 cm. HPLC separations were accomplished using a silica gel column (particle size, 10 μm; column size, 21.2 mm × 250 mm) on a multisolvent delivery system equipped with a refractive index detector connected to a computer that controlled the equipment, data acquisition, processing, and management of the chromatographic information. The ^{1}H (500 MHz), ^{13}C (125.7 MHz), COSY, HMQC, and HMBC experiments were measured in $CDCl_3$ solution using tetramethylsilane as the internal standard. Positive-ion HRFABMS were recorded using a matrix of triethanolamine.

Spicigerolide (1). A natural product isolated from *Hyptis spicigera*. Physical constants and spectroscopic data were identical to those previously reported.[10] The ^{1}H NMR spectral parameters obtained by spectral simulation are listed in Table 2.

Partial Acetylation of Synrotolide. Synrotolide (**9**)[14] (50 mg) was dissolved in a mixture of Ac_2O/pyridine (7.5 μL/250 μL), and the mixture was stirred at −10 °C for 60 min. Then a second addition of Ac_2O/pyridine was done with further stirring at room temperature for 180 min. The reaction mixture was evaporated to dryness under an Ar flow, and the residue was subjected to HPLC (hexane/EtOAc 1:4; flow rate =5 mL/min) yielding 7.5 mg (11.5%) of peracetyl synrotolide (**2**, t_R 20.7 min), 4.8 mg (8.1%) of 5′-acetylsynrotolide (**10**, t_R 25.1 min), 18.5 mg (31.3%) of 4′-acetylsynrotolide (**12**, t_R 26.8 min), and 4.9 mg of starting material (**9**, t_R 35.9 min).

Peracetylsynrotolide (2). Physical constants and spectroscopic data were identical to those previously reported.[14] The ^{1}H NMR spectral parameters obtained by spectral simulation are listed in Table 2.

5′-Acetylsynrotolide (10). Oil, ORD $[\alpha]_{589}$ +1, $[\alpha]_{578}$ +1, $[\alpha]_{546}$ +2, $[\alpha]_{436}$ +15, $[\alpha]_{365}$ +64 (*c* 0.59, $CHCl_3$); ^{1}H NMR 6.89 (ddd, *J* = 9.8, 5.2, 3.2 Hz, H-4), 6.04 (ddd, *J* = 9.7, 2.2, 1.4 Hz, H-3), 5.88 (ddd, *J* = 11.3, 8.1, 1.0 Hz, H-1′), 5.72 (ddd, *J* = 11.3, 9.4, 1.0 Hz, H-2′), 5.53 (ddd, *J* = 9.4, 4.5, 1.0 Hz, H-3′), 5.27 (dddd, *J* = 9.0, 8.1, 7.5, 1.0 Hz, H-6), 5.23 (dq, *J* = 6.5, 3.9 Hz, H-6′), 5.06 (dd, *J* = 7.2, 3.9 Hz, H-5′), 3.92 (ddd, *J* = 7.2, 5.5, 4.5 Hz, H-4′), 2.62 (d, 5.5, OH), 2.48−2.42 (m, 2 H, H-5), 2.12 (s, 3 H, OCOMe), 2.09 (s, 3 H, OCOMe), 2.01 (s, 3 H, OCOMe), 1.28 (d, *J* = 6.5 Hz, CH_3-7′); ^{13}C NMR δ 170.2 (× 2) (OCOMe), 169.9 (OCOMe), 163.3 (C-2), 144.6 (C-4), 132.9 (C-1′), 126.9 (C-2′), 121.5 (C-3), 74.1 (C-6), 72.9 (C-5′), 72.0 (C-4′), 70.2 (C-3′), 69.0 (C-6′), 29.5 (C-5), 21.1 (OCOMe), 21.0 (OCOMe), 20.9 (OCOMe), 14.6 (C-7′); EIMS (20 eV) *m*/*z* 384 $[M]^+$ (0.3), 204 $[384 - 3C_2H_4O_2]^+$ (21), 195 $[384 - C_8H_{13}O_5]^+$ (18), 177 $[195 - H_2O]^+$ (27), 165 (20), 154 (38), 153 (39), 148 (20), 136 (67), 135 $[195 - C_2H_4O_2]^+$ (62), 129 (41), 118 (20), 108 (28), 107 (47). HRFABMS *m*/*z* 407.1315 $[M + Na]^+$ (calcd for $C_{18}H_{24}O_9Na$ requires 407.1313).

4′-Acetylsynrotolide (12). White crystals, mp 152−154 °C, ORD $[\alpha]_{589}$ +1, $[\alpha]_{578}$ +1, $[\alpha]_{546}$ +5, $[\alpha]_{436}$ +18, $[\alpha]_{365}$ +77 (*c* 1.26, $CHCl_3$); ^{1}H NMR 6.90 (ddd, *J* = 9.7, 4.8, 3.5 Hz, H-4), 6.04 (ddd, *J* = 9.7, 1.8, 1.8 Hz, H-3), 5.90 (ddd, *J* = 11.3, 8.1, 0.7 Hz, H-1′), 5.80 (ddd, *J* = 10.0, 2.8, 0.7 Hz, H-3′), 5.73 (ddd, *J* = 11.3, 10.0, 1.1 Hz, H-2′), 5.38 (dddd, *J* = 9.5, 8.1, 7.1, 1.1 Hz, H-6), 5.08 (dd, *J* = 9.3, 2.8 Hz, H-4′), 4.90 (dq, *J* = 6.6, 2.6 Hz, H-6′), 3.80 (ddd, *J* = 9.3, 5.5, 2.6 Hz, H-5′), 2.82 (d, 5.5, OH), 2.49−2.40 (m, 2 H, H-5), 2.12 (s, 3 H, OCOMe), 2.08 (s, 3 H, OCOMe), 2.03 (s, 3 H, OCOMe), 1.24 (d, *J* = 6.6 Hz, H-7′); ^{13}C NMR δ 170.9 (OCOMe), 169.7 (× 2) (OCOMe), 163.6 (C-2), 144.9 (C-4), 132.8 (C-1′), 125.8 (C-2′), 121.3 (C-3), 74.2 (C-6), 72.3 (C-4′), 72.0 (C-6′), 71.2 (C-5′), 68.5 (C-3′), 29.5 (C-5), 21.2 (OCOMe), 20.9 (× 2) (OCOMe), 14.2 (CH_3-7′); EIMS (20 eV) *m*/*z* 384 $[M]^+$ (0.7), 204 $[384 - 3C_2H_4O_2]^+$ (28), 178 (39), 177 (24), 154 (23), 153 (38), 149 (22), 148 (23), 136 (76), 135 (57), 129 (28), 118 (21), 108 (25), 107 (51). HRFABMS *m*/*z* 407.1321 $[M + Na]^+$ (calcd for $C_{18}H_{24}O_9Na$ requires 407.1313).

Oxidation of Monoacetyl Derivatives. 4′-Acetylsynrotolide (**12**, 18 mg) was dissolved in AcOH (800 μL) and treated with CrO_3/H_2O (18 mg/1600 μL) for 2 h. The solution was diluted with H_2O and extracted with Et_2O. The organic phase was worked up as usual. Removal of the solvent left a residue that was analyzed by HPLC (hexane/EtOAc 1:4; flow rate =5 mL/min) to afford 6 mg (33.5%) of 4′-acetyl-5′-oxosynrotolide (**13**, t_R 19.4 min). The same conditions were employed with 5′-acetylsynrotolide (**10**, 5 mg) to yield 3 mg (61%) of 5′-acetyl-4′-oxosynrotolide (**11**).

5′-Acetyl-4′-oxosynrotolide (11). Oil; ORD $[\alpha]_{589}$ +10, $[\alpha]_{578}$ +12, $[\alpha]_{546}$ +29, $[\alpha]_{436}$ +51, $[\alpha]_{365}$ +60 (*c* 0.60, $CHCl_3$); ^{1}H NMR 6.92 (ddd, *J* = 9.8, 5.2, 2.7 Hz, H-4), 6.07 (ddd, *J* = 9.8, 2.6, 1.1 Hz, H-3), 5.96 (ddd, *J* = 11.1, 8.4, 1.1 Hz, H-1′), 5.91 (dd, *J* = 8.8, 1.1 Hz, H-3′), 5.67 (ddd, *J* = 11.1, 8.8, 1.2 Hz, H-2′), 5.61 (d, *J* = 3.9 Hz, H-5′), 5.32 (dddd, *J* = 11.1, 8.4, 5.2, 1.2 Hz, H-6), 5.26 (dq, *J* = 6.6, 3.9 Hz, H-6′), 2.53 (dddd, *J* = 18.5, 5.2, 5.2, 1.1 Hz, H-5eq), 2.45 (dddd, *J* = 18.5, 11.1, 2.7, 2.6 Hz, H-5ax), 2.20 (s, 3 H, OCOMe), 2.19 (s, 3 H, OCOMe), 2.04 (s, 3 H, OCOMe), 1.25 (d, *J* = 6.6 Hz, CH_3-7′). EIMS (20 eV) *m*/*z* 382 $[M]^+$ (1), 165 (34), 153 (18), 149 (32), 148 (48), 135 (32), 115 (21). HRFABMS *m*/*z* 405.1164 $[M + Na]^+$ (calcd for $C_{18}H_{22}O_9Na$ requires 405.1156).

4′-Acetyl-5′-oxosynrotolide (13). Oil; $[\alpha]_{589}$ +10, $[\alpha]_{578}$ +13, $[\alpha]_{546}$ +16, $[\alpha]_{436}$ +30 (*c* 0.30, $CHCl_3$); ^{1}H NMR 6.87 (ddd, *J* = 9.5, 5.5, 2.5 Hz, H-4), 6.03 (ddd, *J* = 9.5, 2.5, 1.0 Hz, H-3), 5.87 (ddd, *J* = 10.0, 3.5, 0.5 Hz, H-3′), 5.85 (dddd, *J* = 11.0, 8.5, 0.5 Hz, H-1′), 5.70 (d, *J* = 3.5 Hz, H-4′), 5.68 (ddd, *J* = 11.0, 10.0, 1.0 Hz, H-2′), 5.32 (dddd, *J* = 11.0, 8.5, 5.0, 1.0 Hz, H-6), 5.27 (q, *J* = 7.0 Hz, H-6′), 2.41 (dddd, *J* = 18.5, 5.5, 5.0, 1.0 Hz, H-5eq), 2.34 (dddd, *J* = 18.5, 11.0, 2.5, 2.5 Hz, H-5ax), 2.18 (s, 3 H, OCOMe), 2.13 (s, 3 H, OCOMe), 2.01 (s, 3 H, OCOMe), 1.36 (d, *J* = 7.0 Hz, CH_3-7′); ^{13}C NMR δ 205.3 (C-5′), 170.5 (OCOMe), 170.0 (OCOMe), 169.8 (OCOMe), 163.6 (C-2), 144.6 (C-4), 133.4 (C-1′), 125.0 (C-2′), 121.5 (C-3), 75.0 (C-4′), 73.8 (C-6), 73.0 (C-6′), 67.3 (C-3′), 29.2 (C-5), 20.8 (OCOMe), 20.7 (OCOMe), 20.5 (OCOMe), 16.1 (C-7′); EIMS (20 eV) *m*/*z* 382 $[M]^+$ (0.2), 165 (40), 153 (24), 149 (40), 148 (53), 147 (31), 136 (20), 135 (36), 115 (23). HRFABMS *m*/*z* 405.1159 $[M + Na]^+$ (calcd for $C_{18}H_{22}O_9Na$ requires 405.1156).

Preparation of Peracetyl-4′-*epi*-synrotolide (3). A solution of 5′-acetyl-4′-oxosynrotolide (**11**, 1.5 mg) in MeOH (500 μL) was treated with a solution of $NaBH_4$/MeOH (500 μg in 500 μL) for 1 h. The reaction mixture was dissolved in water and extracted with EtOAc. The organic phase was worked up as usual. The residue (0.9 mg) was treated with acetyl chloride (100 μL) at room temperature for 90 min. The reaction mixture was evaporated under a N_2 flow and subjected to HPLC (*n*-hexane/EtOAc, 1:1; flow rate = 0.5 mL/min) affording peracetyl synrotolide **2** (0.5 mg, 30.1%) and peracetyl derivative **3** (0.4 mg, 24.1%, t_R = 23.2 min) as a colorless oil, ORD $[\alpha]_{589}$ +18, $[\alpha]_{578}$ +20, $[\alpha]_{546}$ +31, $[\alpha]_{436}$ +42, $[\alpha]_{365}$ +53 (*c* 0.50, $CHCl_3$); ^{1}H NMR (See Table 2); EIMS (20 eV) *m*/*z* 366 $[M - C_2H_4O_2]^+$ (0.5), 230 (40.0), 205 (29), 204 (30), 178 (62), 153 (42), 149 (34), 137 (30), 136 (100), 135 $[366 - C_{10}H_{15}O_6]^+$ (63.3), 129 (91.1), 109 (22.0). HRFABMS *m*/*z* 449.1415 $[M + Na]^+$ (calcd for $C_{20}H_{26}O_{10}Na$ requires 449.1418).

Preparation of Peracetyl-5′-*epi*-synrotolide (4). A solution of 4′-acetyl-5′-oxosynrotolide (**13**, 2 mg) in MeOH (500 μL) was treated with a solution of $NaBH_4$ (500 μg) in MeOH (500 μL) for 1 h. The reaction mixture was dissolved in water and extracted with EtOAc. The organic phase was worked up as usual. The residue (1.9 mg) was treated with acetyl chloride (100 μL) at room temperature for 90 min. The reaction mixture was evaporated under a N_2 flow and subjected to HPLC as above to afford peracetyl synrotolide (**2**, 1.2 mg, 52%) and peracetyl derivative **4** (0.8 mg, 37%, t_R = 23.2 min) obtained as a colorless oil; ORD $[\alpha]_{589}$ +32, $[\alpha]_{578}$ +33, $[\alpha]_{546}$ +48, $[\alpha]_{436}$ +97, $[\alpha]_{365}$ +210 (*c* 0.60, $CHCl_3$); ^{1}H NMR (See Table 2); ^{13}C NMR δ 170.5 (OCOMe), 170.3 (× 2) (OCOMe), 169.4 (OCOMe), 163.6

(C-2), 144.0 (C-4), 134.4 (C-1′), 126.3 (C-2′), 121.8 (C-3), 73.7 (C-6), 71.7 (C-5′), 70.7 (C-4′), 68.6 (C-6′), 66.1 (C-3′), 29.9 (C-5), 21.0 (OCOMe), 20.8 (× 2) (OCOMe), 20.6 (OCOMe), 16.3 (C-7′); EIMS (20 eV) m/z 366 $[426 - C_2H_4O_2]^+$ (0.7), 230 (40), 205 (20), 204 (65), 178 (69), 165 (30), 159 (23), 153 (55), 149 (24), 137 (27), 136 (100), 135 $[426 - C_{10}H_{15}O_6 - C_2H_4O_2]^+$ (75), 130 (23), 129 (66), 118 (39), 117 (23), 108 (31), 107 (43). HRFABMS m/z 449.1395 $[M + Na]^+$ (calcd for $C_{20}H_{26}O_{10}Na$ requires 449.1418).

Extraction and Isolation of *epi*-Olguine and Deacetyl-*epi*-olguine. The entire plant of *Hyptis spicigera* with inflorescences and fruits were collected in Municipio Emiliano Zapata, Dos Ríos (at 940 m. a.s.l.), Veracruz, Mexico in November 2009. The plant was identified by one of us (A.C.H.-R.) and a voucher specimen (Hernández-Rojas 118) was deposited in the herbarium of the Instituto de Ecología, Xalapa, Veracruz, Mexico (accession number XAL0000246). Also, voucher specimens were archived at the Departamento de Farmacia, Facultad de Química, Universidad Nacional Autónoma de México (sample code: HR-118-XAL) and in the botanical Collection of Facultad de Ciencias, Universidad Nacional Autónoma de México (voucher 127318). The air-dried whole plant of *H. spicigera* (1400 g) was ground and extracted with $CHCl_3$ overnight (4 × 6 L). The macerate was concentrated in vacuo (54 g) and fractionated using silica gel vacuum-liquid chromatography eluting with hexane/$CHCl_3$, $CHCl_3$/Me_2CO, and Me_2CO/MeOH. The column was then washed with 100% MeOH. Altogether, 10 pooled fractions were collected (80 fractions, 500 mL each). Fraction F5 (500 mg, eluted with $CHCl_3$/Me_2CO) was resolved by HPLC on silica column with an isocratic elution of hexane/AcOEt (1:1) and a flow rate of 9 mL/min. Eluates across the peaks with t_R values of 13.9 min (peak I), and 17.1 min (peak II) were collected by the technique of heart cutting and independently reinjected (sample injection 500 μL, concentration 0.1 mg/mL) in the apparatus operating in the recycle mode to achieve total homogeneity after six consecutive cycles employing the same instrumental conditions described above. These techniques afforded compound **14** (236 mg) from peak I and compound **15** (100 mg) from peak II.

5′-*epi*-Olguine (14). Natural product isolated from *Hyptis spicigera* (see Supporting Information); mp 75−76 °C; ORD $[\alpha]_{589}$ +127, $[\alpha]_{578}$ +133, $[\alpha]_{546}$ +153, $[\alpha]_{436}$ +286, $[\alpha]_{365}$ +521 (*c* 0.29, $CHCl_3$). NMR data were identical to those previously reported.[21]

5-Deacetoxy-5′-*epi*-olguine (15). Natural product isolated from *Hyptis spicigera* (see Supporting Information); mp 147−149 °C; ORD $[\alpha]_{589}$ −64, $[\alpha]_{578}$ −67, $[\alpha]_{546}$ −76, $[\alpha]_{436}$ −122 (*c* 0.1, $CHCl_3$). NMR data were identical to those previously reported.[22]

Molecular Modeling Calculations. Molecular building and the initial conformational search were carried out in the Spartan '04 program[24] using the MMFF94 force-field calculation. The conformational search was performed through a systematic search protocol in which the torsion angles C(2′)−C(3′)−C(4′)−C(5′), C(3′)−C(4′)−C(5′)−C(6′), and C(4′)−C(5′)−C(6′)−C(7′) in the heptenyl moiety were rotated in steps of 120°, starting at 60° for each central bond, and the torsion angles of the C(1′)═C(2′)−C(3′)−C(4′) and C(5)−C(6)−C(1′)═C(2′) dihedral angles were rotated in steps of 180°, generating a total of 108 initial conformers for each stereoisomer (**1**−**8**) with a overall total number of conformers of 864. The acetyloxy H−C_{sp3}−O−C_{sp} and C_{sp3}−O−C═O dihedral angles were initially set to 0° and explored within a rage from +60° to −60°. Molecular potential energy of all structures was minimized to an rmsd gradient of 1×10^{-6} kcal/mol on the potential energy surface. Some out of the 108 conformers achieved for each stereoisomer were ruled out due of severe intramolecular hindering steric interactions. The remaining conformers of **1**−**8** (83, 99, 100, 97, 89, 94, 59, and 66, respectively) were geometrically optimized without restrictions using the hybrid density functional theory (B3LYP) method in conjunction with the DGDZVP basis set. The stationary points (optimized structures) were used to calculate the thermochemical parameters, and the IR frequencies were estimated at 298 K and 1 atm. Magnetic shielding tensors were calculated with the gauge-including atomic orbital (GIAO) method, and total NMR spin−spin coupling constants (SSCC) *J* (Hz) were calculated as the summation of the Fermi contact (FC), diamagnetic spin−orbit (DSO), spin-dipolar (SD), and paramagnetic spin−orbit (PSO) which were calculated from B3LYP/DGDZVP optimized structures by using the *spinspin* option during the NMR jobs. All DFT calculations, including NMR, were carried out with the Gaussian 03 program on a Linux operating system loaded in a cluster, which includes 1368 processors at 2.6 GHz and a RAM memory of 3 terabytes. For each job, a maximum of four processors was used and each conformer required three different DFT jobs: geometric optimizations, frequency calculations, and SSCC estimations. The total CPU time consumed in this work was approximately 5×10^4 h. The Gibbs free energy equation ($\Delta G = -RT \ln K$) was used to obtain the conformational population, taking into account a cyclic equilibrium at 298 K between the selected conformers of **1**−**8** (9, 21, 29, 12, 10, 10, 25, and 13, respectively) within a 0.0−3.0 kcal/mol range with respect to each global minimum. The Gibbs free energy values $\Delta G°$ were obtained from the vibrational frequency calculations as the sum of electronic and thermal free energies. Calculations using the triple-zeta basis set DGTZVP were also carried out with the nine minimum energy conformers of spicigerolide (**1**) affording similar total energy values as those obtained with DGDZVP basis set, but emphasizing the free energy differences. The calculated coupling constant values were essentially similar, leading to practically the same results. The calculation time using DGTZVP was considerably higher (almost twice the total CPU time) than that consumed with DGDZVP (see Table S32 in Supporting Information).

Spectral Simulation. All experimental $^3J_{HH}$ were obtained by nonlinear fit of the ^{1}H NMR spectrum to the spectral parameters using the MestRe-C 3.0 program (Mestrelab Research, Santiago de Compostela, Spain).

■ ASSOCIATED CONTENT

Supporting Information. NMR spectra of compounds **1**−**4** and **10**-**13**. Relevant conformers and simulated vs experimental spectra of **14** and **15**. DFT B3LYP/DGDZVP total free energies, population, and DFT ^{1}H−^{1}H coupling constants of stereoisomers **1**−**8** and **14**−**17**. Calculated IR frequencies and NMR shielding tensors of stereoisomers **1**−**8**, calculated H−C−C−H dihedral angles, DFT B3LYP/DGTZVP energies, and DFT B3LYP/DGTZVP ^{1}H−^{1}H coupling constants of **1**. This material is available free of charge via the Internet at http://pubs.acs.org.

■ AUTHOR INFORMATION

Corresponding Author
*E-mail: ccerda@cinvestav.mx; pereda@servidor.unam.mx.

■ ACKNOWLEDGMENT

This research was partially supported by Consejo Nacional de Ciencia y Tecnología (grant 104887). F.L.-V. and G.A.S.-O. are grateful to CONACyT for postgraduate and graduate student scholarships, respectively. Authors are deeply indebted to Professor Michael T. Davies Coleman, Rhodes University, Grahamstown, South Africa for his generous donation of synrotolide. Thanks are due to Georgina Duarte and Margarita Guzmán (Facultad de Química, UNAM) for recording mass spectra. Geometry optimizations and coupling constant calculations were

performed in the KanBalam computer cluster at Departamento de Supercómputo, Dirección General de Servicios de Cómputo Académico, UNAM.

REFERENCES

(1) Bifulco, G.; Dambruoso, P.; Gomez-Paloma, L.; Riccio, R. *Chem. Rev.* **2007**, *107*, 3744–3779.

(2) Folkers, G.; Yarim, M; Pospisil, P. In *Chirality in Drug Research*; Francotte, E., Lindner, W., Eds.; Wiley-VCH Verlag: Weinheim, 2006; Vol. 33, pp 323−340.

(3) (a) Sarotti, A. M.; Pellegrinet, S. C. *J. Org. Chem.* **2009**, *74*, 7254–7260. (b) Smith, S. G.; Goodman, J. M. *J. Org. Chem.* **2009**, *74*, 4597–4607.

(4) Mendoza-Espinoza, J. A.; López-Vallejo, F.; Fragoso-Serrano, M.; Pereda-Miranda, R.; Cerda-García-Rojas, C. M. *J. Nat. Prod.* **2009**, *72*, 700–708.

(5) Tuttle, T.; Kraka, E.; Wu, A.; Cremer, D. *J. Am. Chem. Soc.* **2004**, *126*, 5093–5107.

(6) Klepach, T. E.; Carmichael, I.; Serianni, A. S. *J. Am. Chem. Soc.* **2005**, *127*, 9781–9793.

(7) (a) Bagno, A.; Rastrelli, F.; Saielli, G. *Chem.—Eur. J.* **2006**, *12*, 5514–5525. (b) Manzo, E.; Gavagnin, M.; Bifulco, G.; Cimino, P.; Di Micco, S.; Ciavatta, M. L.; Guo, Y. W.; Cimino, G. *Tetrahedron* **2007**, *63*, 9970–9978. (c) Galasso, V.; Kovac, B.; Modelli, A. *Chem. Phys.* **2007**, *335*, 141–154. (d) Plaza, A.; Piacente, S.; Perrone, A.; Hamed, A.; Pizza, C.; Bifulco, G. *Tetrahedron* **2004**, *60*, 12201–12209.

(8) (a) Davies-Coleman, M. T.; Rivett, D. E. A. Naturally occurring 6-substituted 5,6-dihydro-α-pyrones. In *Progress in the Chemistry of Organic Natural Products*; Herz, W., Grisebach, H., Kirby, G. W., Tamm, Ch., Eds.; Springer: New York, 1989; Vol. 55, pp 1−35. (b) Collet, L. A.; Davies-Coleman, M. T. Rivett, D. E. A. Naturally occurring 6-substituted 5,6-dihydro-α-pyrones. In *Progress in the Chemistry of Organic Natural Products*; Herz, W., Falk, H., Kirby, G. W., Moore, R. E., Tamm, Ch., Eds.; Springer: New York, 1998; Vol. 75, pp 182−209.

(9) (a) Pereda-Miranda, R.; Hernández, L.; Villavicencio, M. J.; Novelo, M.; Ibarra, P.; Chai, H.; Pezzuto, J. M. *J. Nat. Prod.* **1993**, *56*, 583–593. (b) Pereda-Miranda, R. In *Bioactive Natural Products from Traditionally Used Mexican Plants*; Arnason, J. T., Mata, R., Romeo, J. T., Eds.; *Phytochemistry of Medicinal Plants*; Plenum: New York, 1995; pp 83−112. (c) Fragoso-Serrano, M.; Gibbons, S.; Pereda-Miranda, R. *Planta Medica* **2005**, *71*, 278–280.

(10) Pereda-Miranda, R.; Fragoso-Serrano, M.; Cerda-García-Rojas, C. M. *Tetrahedron* **2001**, *57*, 47–53.

(11) Hoffmann, H. M. R.; Rabe, J. *Angew. Chem., Int. Ed.* **1985**, *24*, 94–110.

(12) (a) Usui, T.; Watanabe, H.; Nakayama, H.; Tada, Y.; Kanoh, N.; Kondoh, M.; Asao, T.; Takio, K.; Watanabe, H.; Nishikawa, K.; Kitahara, T.; Osada, H. *Chem. Biol.* **2004**, *11*, 799–806. (b) Yoshida, M.; Matsui, Y.; Ikarashi, Y.; Usui, T.; Osada, H.; Wakasugi, H. *Anticancer Res.* **2007**, *27*, 729–736.

(13) (a) Falomir, E.; Murga, J.; Ruiz, P.; Carda, M.; Marco, A.; Pereda-Miranda, R.; Fragoso-Serrano, M.; Cerda-García-Rojas, C. M. *J. Org. Chem.* **2003**, *68*, 5672–5676. (b) Falomir, E.; Murga, J.; Carda, M.; Marco, A. *Tetrahedron Lett.* **2003**, *44*, 539–541. (c) Georges, Y.; Ariza, X.; Garcia, J. *J. Org. Chem.* **2009**, *74*, 2008–2012. (d) Chakraborty, T. K.; Purkait, S. *Tetrahedron Lett.* **2008**, *49*, 5502–5504. (e) Srihari, P.; Kumar, P.; Subbarayudu, K.; Yadav, J. S. *Tetrahedron Lett.* **2007**, *48*, 6977–6981. (f) Krishna, R. P.; Reddy, S. *Tetrahedron* **2007**, *63*, 3995–3999. (g) García-Fortanet, J.; Murga, J.; Carda, M.; Marco, J. A. *Arkivoc* **2005**, 175–188.

(14) Davies-Coleman, M. T.; English, R. B.; Rivett, D. E. A. *Phytochemistry* **1987**, *26*, 1497–1499.

(15) Díez, E.; Casanueva, J.; San Fabián, J.; Esteban, A. L.; Galache, M. P.; Barone, V.; Peralta, J. E.; Contreras, R. H. *Mol. Phys.* **2005**, *103*, 1307–1326.

(16) (a) Masamune, S.; Ma, P.; Moore, R. E.; Fujiyoshi, T.; Jaime, C.; Osawa, E. J. *Chem. Soc., Chem. Commun.* **1986**, 261–263. (b) Osawa, E.; Imai, K.; Fujiyoshi-Yoneda, T.; Jaime, C.; Ma, P.; Masamune, S. *Tetrahedron* **1991**, *47*, 4579–4590. (c) Horton, D.; Wander, J. D. *Carbohydr. Res.* **1970**, *15*, 271–284. (d) Velasco, D.; Castells, J.; López-Calahorra, F.; Jaime, C. *J. Org. Chem.* **1990**, *55*, 3526–3530. (e) Mills, J. A. *Aust. J. Chem.* **1974**, *27*, 1433–1446. (f) López-Calahorra, F.; Velasco, D.; Castells, J.; Jaime, C. *J. Org. Chem.* **1990**, *55*, 3530–3536.

(17) (a) Desiraju, G. R. *Chem. Commun.* **2005**, 2995–3001. (b) Steiner, T. *Chem. Commun.* **1997**, 727–734. (c) Steiner, T. *Angew. Chem., Int. Ed.* **2002**, *41*, 48–76.

(18) Kroon, J.; Kanters, J. A.; Van Duijneveldt-Van de Rijdt, J. G. C. M.; Van Duijneveldt, F. B.; Vliegenthart, J. A. *J. Mol. Struct.* **1975**, *24*, 109–129. (b) Ceccarelli, C.; Jeffrey, G. A.; Taylor, R. *J. Mol. Struct.* **1981**, *70*, 255–271.

(19) Taylor, R; Kennard, O. *J. Am. Chem. Soc.* **1982**, *104*, 5063–5070.

(20) Kroon, J.; Kanters, J. A. *Nature* **1974**, *248*, 667–669.

(21) Lu, G.-H.; Wang, F.-P.; Pezzuto, J. M.; Tam, T. C. M.; Williams, I. D.; Che, C.-T. *J. Nat. Prod.* **1997**, *60*, 425–427.

(22) (a) Delgado, G.; Pereda-Miranda, R.; Romo de Vivar, A. *Heterocycles* **1985**, *23*, 1869–1872. (b) Pereda-Miranda, R.; García, M.; Delgado, G. *Phytochemistry* **1990**, *29*, 2971–2974.

(23) Alemany, A.; Márquez, C.; Pascual, C.; Valverde, S.; Perales, A.; Fayos, J.; Martínez-Ripoll, M. *Tetrahedron Lett.* **1979**, 3579–3582.

(24) Kong, J.; White, C. A.; Krylov, A. I.; Sherrill, C. D.; Adamson, R. D.; Furlani, T. R.; Lee, M. S.; Lee, A. M.; Gwaltney, S. R.; Adams, T. R.; Ochsenfeld, C.; Gilbert, A. T. B.; Kedziora, G. S.; Rassolov, V. A.; Maurice, D. R.; Nair, N.; Shao, Y.; Besley, N. A.; Maslen, P. E.; Dombroski, J. P.; Daschel, H.; Zhang, W.; Korambath, P. P.; Baker, J.; Byrd, E. F. C.; Van Voorhis, T.; Oumi, M.; Hirata, S.; Hsu, C.-P.; Ishikawa, N.; Florian, J.; Warshel, A.; Johnson, B. G.; Gill, P. M. W.; Head-Gordon, M.; Pople, J. A. *J. Comput. Chem.* **2000**, *21*, 1532–1548.